

Capability Enhancement of DC-Link Voltage in a Single-Stage Grid-Connected Photovoltaic Power System

Ayman Alhejji*

* Department of Electrical and Electronics Engineering Technology, Yanbu Industrial College, Yanbu Industrial City, Saudi Arabia

Yanbu Industrial College, Yanbu Industrial City 41912, Saudi Arabia, Tel: +966143946111, Fax: +966143920213, alhejji@rcyci.edu.sa

Received: 21.01.2020 Accepted:27.02.2020

Abstract- This article introduces a new approach for the grid-connected single-stage three-phase photovoltaic (PV) inverter in distribution network. This approach aims at improving the voltage profile at point of common coupling (PCC) between the PV power system and the grid. This improvement is achieved by regulating a dc-link voltage based maximum power point tracking (MPPT). This MPPT is fully utilized for updating the dc-link voltage reference (DLVR) according to environmental conditions. The updated DLVR is compared to the dc-link voltage through adaptive reference integral-proportional (ARPI) controller to develop reference direct current axis and to generate desired inverter pulses under normal and abnormal conditions. To verify the validity of the new approach, simulation results for multiple scenarios such as various environmental conditions alone, various environmental conditions with simultaneous three-phase faults and various environmental conditions with simultaneous voltage dips/sags are obtained from 250-kW single-stage grid-connected PV system. These obtained results illustrate the efficacy of the ARPI controller outperforms the conventional PI controller under all scenarios.

Keywords ARPI controller, Perturb and observe-based MPPT, DC-Link, Single-Stage, Three-Phase Inverter, Grid-connected.

1. Introduction

Solar energy is one of the renewable energy resource solutions used to combat global energy crises [1]. Solar energy in the form of the photovoltaic (PV) module technology has been a growing interest in many applications due to its less maintenance, freedom from noise, freedom from pollution, abundantly accessibility in nature, and affordability along with increasing efficiency of the PV module as reported in [2-5]. In accordance with the system size [2], PV systems are categorized into small scale, intermediate scales, and large scale. Both small- and intermediate-scales PV systems are exploited to supply electrical energy locally, whereas the large-scale or utility-scale PV system delivers electrical energy to the distribution network or auxiliary services. As pointed out in [3], the two stages required additional power electronic components which are expensive include a dc-dc converter along with MPPT and dc-ac inverter in order to inject sinusoidal current into grid [3]. Moreover, additional measurements in two-stage topology are needed like current and voltage measurement as well as logic processes in order to determine MPPT in dc-dc converter in real-time, while dc-ac inverter is

responsible for injecting the sinusoidal current into the grid. These make remarkable indication for the drawback of two-stage PV inverter. Conversely, the proposed single-stage PV inverter will be discussed in literature.

With the increasing demand for electricity, the PV system with the grid integration into distribution system, called-PV array based-distributed generations, has become prevalent. Therefore, a grid-connected PV inverter can be modeled in term of installations such as multistring, centralized and centralized with different maximum power point tracking (MPPT) controllers as addressed in [4]. For example, multistring topology was particularly implemented for utility-scale PV system along with two-level control for direct current boost interface [2]. However, in regard to ample energy production, various renewable energy sources, such as solar, wind and hydro is highly dependent upon seasonal weather variations [5]. As pointed out in [6], it is increasingly significant to determine possible solutions for the issues of power flow and quality in PV systems integrated with grid. In [7], the study was dedicated to accomplishing better transient and steady-state performance through a dc-link voltage controller-based adaptive network based fuzzy inference system. In [8], a great effort has been

dedicated to investigating ample solutions through various reactive current controls. Similarly, an interesting solution approach to solve the issue of power quality has been addressed by [9]. Furthermore, the study in [10] was explicitly focused more on adaptive control of reactive power compensation to enhance the power quality in distribution system along with large scale PV systems. In [5-6,7-8], the study was dedicated to accomplishing better transient and steady-state performance through a dc-link voltage controller using adaptive fuzzy inference.

Different advanced MPPT control techniques [11-20] have been proposed aimed at simply extracting the maximum energy production from the specified capacity in PV system [10]. These techniques of MPPT such as perturb and observe (P&O) [12-13], incremental conductance (IC) algorithm [13-14], parasitic capacitance algorithm [15], and optimization of constant voltage [16] are commonly applied to obtain MPPT from output PV power to meet the load or grid demands. Also, Hybrid MPPT techniques, including P&O, IC and constant voltage were performed and compared in PV system [17] to leverage speed and accuracy in tracking power in partial shading and sudden weather variations. Moreover, artificial intelligence techniques, including MPPT controller using fuzzy logic along with ANN which are mostly combined with the previous conventional MPPT methods in the literature to accurately improve the tracking speed [17-20]. For instance, a MPPT-based on genetic algorithms to deal with nonlinear objective function is provided in [18]; a fuzzy logic (FC)-based MPPT controller is addressed in [19]. A cuckoo search optimization technique has been successfully employed in optimizing proportional-integral control parameters to attain desirable maximum PV power [20]. Moreover, the cuckoo search method was used for MPPT of PV plus hybrid power system [21]. Reference [22] introduced an artificial neural network (ANN)-based MPPT controller. As pointed out in [23], a variable step length of the MPP using incremental conductance was revealed in to increase the output PV power efficiency and stability through a single-stage inverter.

A proportional-integral (PI) controller in voltage control is commonly practiced and advantageous for voltage stability, but the typical PI controller design depends mainly upon the trial and error approach, or a long computation process using optimization as an off-line tuning [20-21], [24-27], and therein lies the cause of its ineffectiveness compared with an adaptive controller. Many trials were introduced for turning out PI controller into adaptive PI. As provided in [28], the ANN scheme was applied to convert the PI controller into an adaptive PI controller. This conversion from the PI controller to the adaptive PI controller using ANN requires some training data and computational experience. The adaptive control technique without adapting or updating the PI controller is the key solution for the PI-based ANN. A model reference adaptive control (MRAC) was introduced and compared with the PI controller as in [29]. However, selecting a reference model poses a big challenge in the MRAC.

A single-stage PV inverter merits further exploration, where the power flow has less power loss and higher power

efficiency due to the lack of a dc/dc converter module. For example, a robust phase-lock loop (PLL) less control is used for a single-stage single-phase on-grid PV multifunctional inverter for promoting power quality by reducing losses in the distribution line and the transformer under grid faults [30]. Reference [31] has proposed an inverter control scheme as a solution to improve power quality through trade-offs between current harmonics and power ripples under grid faults. As pointed out in [32], the single-stage topology has promoted the power produced under partial shading status by enhancing MPPT capability, which leads to superior energy. Similarly, the dc-link voltage enhancement along with reactive power compensation using a feedback linearization technique in PV system was provided in [33]. Likewise, in [34], an active power decoupling control of dual-bulk inverter design aims at directly controlling the dc-link voltage. Hence, the dc-link voltage is desirably equal to the output PV voltage in particular with single-stage inverter. Reference [35] has analyzed the dc-link voltage stability of a single-stage PV system integrated with weak grid. Moreover, as addressed in [36], a current limit control and different dc-link voltage controls were designed and implemented in single-stage on-grid PV inverter in case of grid faults. The same control methods were implemented in a two-stage on-grid PV inverter for more investigations. With more PV power supplies, the negative higher impact on the dc-link occurs, and thus reduces a stability margin of the inverter.

In grid side, short-circuit fault is considered one of the quality power disturbances. Fault ride-through (FRT) has been addressed in [25,36-38] and overcome grid faults events. In [39], the control mechanism applied the reactive power compensation with supercapacitor energy storage system which is integrated with on-grid PV system through bi-directional buck-boost converter. Then, the dc-link of supercapacitor coordinates to inject active and reactive powers into the grid to fulfil FRT requirement. However, the drawbacks of the proposed control mechanism are costly and unreliable in operation. In [40], the study also presented the FRT in order to overcome overvoltage and overcurrent securely and save power electronic components from damage.

Likewise, voltage dip, namely voltage sag, is another feature of quality power disturbance in which the voltage drops from 10% to 90 % of its magnitude [41]. For example, many research studies [43] have discussed low voltage ride-through to overcome the grid faults and protect the PV system from disconnection through the voltage dip. In [45], an adaptive control scheme was effectively promoting the two-stage on-grid PV inverter output from high dc-link voltage issue during voltage dip.

The dc-link voltage of single-stage PV inverter needs a desired range according to [46]. To that end, the desired range of the dc-link voltage simply will curtail current ripple and control dc voltage in dc-link when being chosen as close as its maximum output voltage of the PV array. Even though dc-link voltage control and point of common coupling (PCC) voltage have been enhanced in recent years, most improvements have been achieved by [33-36]. Nonetheless, it is possible to further improve dc-link voltage performance and PCC voltage with adaptive control method in single-

stage PV inverter. Also, all existing literature studies of single-stage PV inverter have not discussed adaptive controller to overcome the following challenges.

- Overvoltage in dc-link of single-stage inverter
- Improving PCC voltage profile during different disturbance scenarios

With this goal, the control approach aims at improving the voltage profile at PCC between the PV power system and the grid. This improvement is achieved by regulating the dc-link voltage that is based on MPPT. This MPPT is fully utilized for updating the dc-link voltage reference (DLVR) according to environmental conditions. The updated DLVR is compared to the actual dc-link voltage through adaptive reference integral-proportional (ARPI) controller to develop reference direct current axis and to generate desired inverter pulses under normal and abnormal conditions. To verify the validity of the proposed approach, simulation results for multiple scenarios such as various environmental conditions alone, various environmental conditions with simultaneous three-phase faults and various environmental conditions with simultaneous voltage dips/sags on 250-kW single-stage grid-connected PV system. The obtained results illustrate the efficacy of the ARPI controller compared with the conventional PI controller.

The rest of the paper is prearranged as follows. Section II will discuss system description; Section III is devoted to dc-link voltage control. Simulation results along with discussions are presented in Section IV; the conclusion is reported in Section V.

2. System Description

The schematic of a proposed grid connected single-stage PV system is depicted in Fig. 1; this system comprises PV array, dc-link capacitors, 3-level inverter, filter and utility grid.

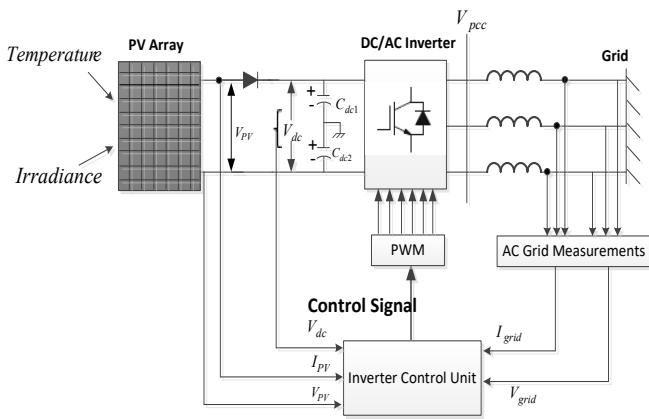


Fig. 1. Feature of the single-stage grid-connected PV system.

The PV system is directly linked across the dc-link capacitance of inverter as shown in Fig.1. Therefore, both output PV voltage reference and dc-link voltage reference are equal as addressed in [30]. Also, a control unit of the inverter scheme comprises the MPPT control scheme, voltage control

scheme and current control scheme, phase locked loop (PLL) synchronization, and a pulse width modulation (PWM) generator. In the inverter control unit, the output PV voltage and current are directly connected to the MPPT control scheme, and the output MPPT control is utilized as dc-link voltage reference for voltage control. Hence, the three-phase inverter stabilizes the dc-link voltage, and then synchronizes the voltage and frequency with grid in order to transfer AC power into the grid.

2.1. Photovoltaic Module

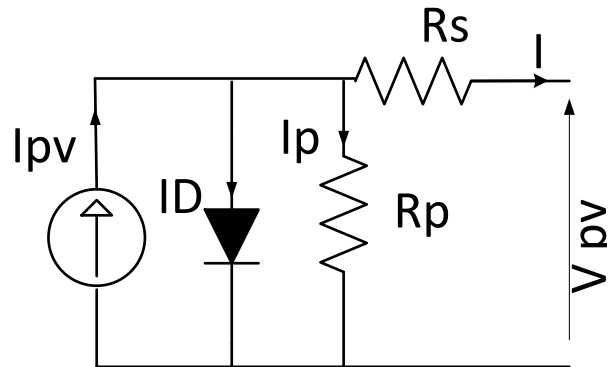


Fig. 2. Equivalent circuit of the photovoltaic module

$$I = n_p I_{pv} - n_p I_o \left[\exp \left(\frac{V_{PV} + I.R_s \left(\frac{n_s}{n_p} \right)}{V_T} \right) - 1 \right] - \frac{V_{PV} + I.R_s \left(\frac{n_s}{n_p} \right)}{R_p \left(\frac{n_s}{n_p} \right)} \tag{1}$$

where I_{PV} expresses the photovoltaic current based on solar irradiance and temperature conditions; I_D represents the current passing through diode, and I_p denotes the current passing through parallel resistors, and V_{PV} denotes the output voltage of the photovoltaic module. In addition, R_p and R_s express the parallel and series resistors, respectively. Additionally, n_p and n_s are numbers of parallel and series connections, respectively. I_o is the reverse saturation current. In addition, $V_T = n_s kT / q$ is the thermal voltage of the photovoltaic module, $k = 1.3805 \times 10^{23} J / K$ is Boltzmann's constant, and $q = 1.60217646 \times 10^{19} C$ defines the electron charge.

Table 1. Specifications of the PV Array.

Parameters	Values
Rated PV power	414.8 W
Open circuit voltage	85.3 V
Short-circuit current	6.09 A

MPPT voltage	72.9 V
MPPT current	5.69 A
Number of series modules	7
Number of parallel strings	8
Series resistor	0.537Ω
Parallel resistor	419.78 Ω
Voltage-temperature coefficient	-0.229°C
Current-temperature coefficient	-0.030706°C

2.2. Maximum Power Point Tracking Module

According to a research study in [42], the P&O-based MPPT implemented in single-stage micro-inverter guarantees the 0.98 power factor of the system, 4.7% total current distortion (THD), and 93% efficiency of the inverter. The V-I and P-V nonlinear characteristics of PV arrays connected in 7 series modules and 88 parallel strings are plotted at 25°C temperature and an irradiance of 1000 W/m², as shown below in Fig.3.

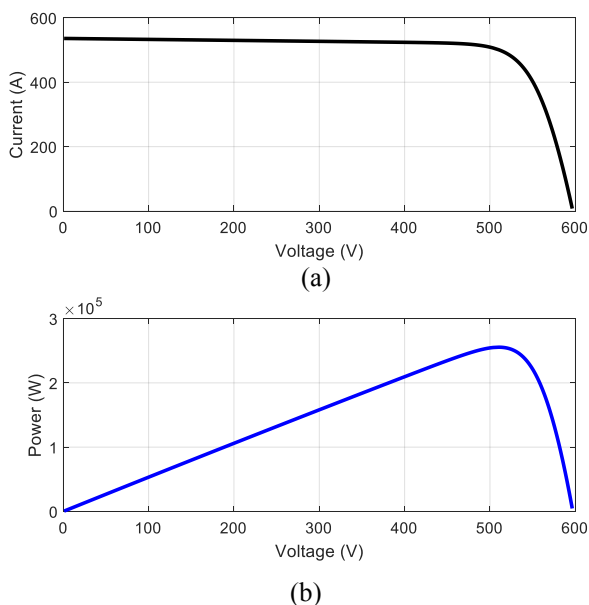


Fig. 3. (a) I-V characteristics, and (b) P-V characteristics of the output PV panel.

The P&O based-MPPT technique in [12] is used in this paper to estimate the DLVR for the voltage control. A proposed range of the DLVR as generated from the P&O

based-MPPT technique has been set between 357 volts and 583 volts because the nominal value of dc-link voltage is 480 volts. If the dc-link voltage is increased beyond that maximum limit, it could lead dc-link to damage, conversely, if the dc-link voltage is decreased, then the dc-link disconnects the PV system from the grid.

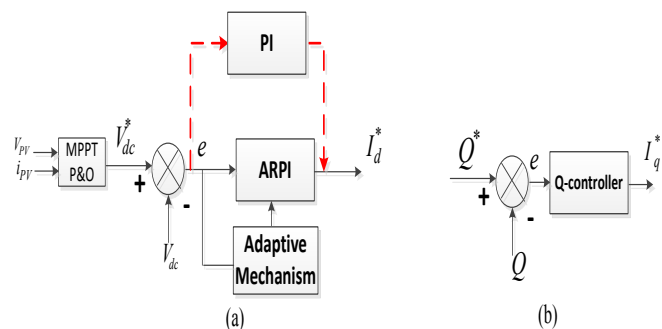
2.3. Single Stage Inverter

A control block diagram of a single-stage three-level inverter is seen in Fig.4. A control unit completely includes, P&O-based MPPT output, voltage control, reactive power control, PLL synchronization feature, and current control to regulate the three-phase IGBT switching of the inverter. This single-stage inverter is deployed to stabilize the dc-link voltage, and then generate pulses of three-level IGBT switches and the PCC voltage with field-oriented control as shown below in Fig.4.

As given in [12], the mathematical model of the inverter is expressed as

$$\begin{aligned}
 V_d &= R_g i_d + L_o \frac{di_d}{dt} + \omega_f L_o i_q + V_{id} \\
 V_q &= R_g i_q + L_g \frac{di_q}{dt} + \omega_f L_o i_d + V_{iq} \quad (2) \\
 P_{grid} &= 1.5 V_d i_d \\
 Q_{grid} &= 1.5 V_q i_q
 \end{aligned}$$

where V_d and V_q describe the d-q axis components of the grid voltage; V_{id} and V_{iq} denote the d-q axis components of inverter voltages. Additionally, i_d and i_q in the d-q axis describe the grid current, and ω_f defines the angular frequency [rad/sec]. Furthermore, R_g and L_o represent the resistance and inductance of the grid, respectively. Also, P_{grid} defines the active power in watts, and Q_{grid} represents the reactive power in var.



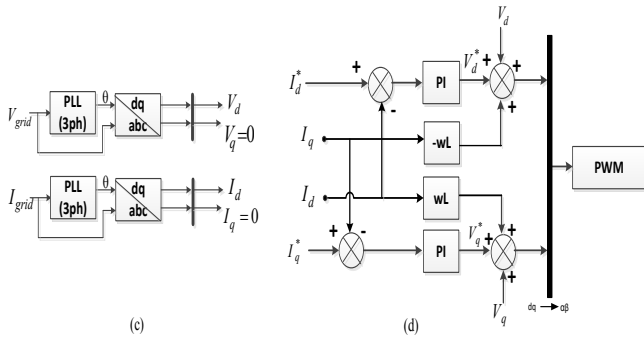


Fig. 4. Block diagram of single-stage inverter. A) schematic diagram of voltage control loop; b) schematic diagram of Q-control where its output is set to be zero; c) schematic diagram of transformation module; d) schematic diagram of current control loop.

Under the MPPT operation, a variable step is improved in P&O based-MPPT controller whereby it adapts different step length values by increasing or decreasing the voltage with consideration for the range of the DLVR $357 < V_{dc}^* < 583$. This range of the DLVR is utilized as the set point for the voltage control scheme. As represented in Fig.4a, the duty cycle of the output P&O-based MPPT is feed-forward and fully utilized as V_{dc}^* for the voltage control scheme to produce the current reference of the d-axis component i_d^* which directly regulates the active power flow into the grid whereas a quadrature axis component of the current reference i_q^* in Fig.4b is always set to be zero in normal operation at unity power factor because it controls the reactive power compensation to the grid in case of abnormal operation. In Fig.4c, the grid synchronization is significant for PV system integration with the grid because a current injected into the grid requires synchronization with grid voltage with the existence of a phase-locked loop for providing a grid phase angle [36]. By applying the park transformation, the reference frame transformation module in Fig.4c helps transform three-phase voltage and current waveforms into d-q axis components synchronously rotating with grid voltage. Moreover, in three-level three-phase twelve-IGBT switch inverter, an inner control loop scheme as seen in Fig.4d plays an important role for generating the output voltage reference of the d-q axis components. These the d-q axis components of the voltage references are converted to three-phase voltage, and then they are added with a triangular signal to produce the firing pulses of IGBT switches.

3. DC link Voltage Control

Numerous control techniques such as [5],[9]-[10] and [23]-[26] have been proposed and implemented to effectively stabilize the dc-link voltage. Owing to abnormal conditions such as environmental changes, short-circuit faults and voltage dips in the PV power system plant, the solutions for the control problems have increasingly been enhanced, especially for dc-link control to hold the best power stability

between the generated power and the grid power. With the regulation of the d-axis current reference as represented in Fig.4a, the dc-link voltage control in the single-stage inverter can be successfully achieved and the injection of active power can be controlled accordingly.

3.1. Adaptive Proportional-Integral Controller Design

If no control action is performed during the voltage dip, then the PV power increases higher than the active power in grid side. Hence, the dc-link voltage increases to undesired amplitude which could lead to component failure.

Consider the mathematical dc-link model as follows

$$\frac{1}{2} C \frac{dV_{dc}^2}{dt} = P_{pv} - P_{grid} \quad (3)$$

For simplicity, output PV power is $P_{pv} = i_{pv} \times v_{pv}$ in watts and the grid power is $P_{grid} = 1.5 \times v_d i_d$ in watts. Let us further simplify the dc-link structure as

$$C \frac{dV_{dc}}{dt} = i_{pv} - 1.5 \frac{v_d}{v_{dc}} i_d \quad (4)$$

where C expresses the dc-link capacitor, P_{pv} , i_{pv} , and v_{pv} are the output PV power in watts, output PV current in Amps, and output PV voltage in volts, respectively. Moreover, i_d is a direct current axis in amperes to control the active power in grid side. V_d describes the direct axis of the grid voltage. V_{dc} denotes a dc-link voltage that aims at maintaining the best balance between generation and grid.

The error of the dc-link voltage is given by

$$e = V_{dc}^* - V_{dc} \quad (5)$$

where V_{dc}^* and V_{dc} denote the DLVR and dc-link voltage, respectively. As shown in (4), the d-axis component of the grid current, i_d , directly controls the active power P to the grid, and the q-axis component of the grid current, $i_q = 0$, is always set zero and directly controls the reactive power injection into the grid. The d-axis component of current reference i_d^* is produced from the PI voltage controller used in dc-link voltage regulation as follows

$$i_d^* = K_p e + K_I \int e dt \quad (6)$$

However, the fixed gains of the PI controller lead to a slow response and ripples in controlled dc-link voltage. Therefore, the proposed ARPI is used for dc-link voltage regulation to improve the performance of the dc-link voltage with less overshoot and low ripples. The ARPI control structure is given as follows:

$$i_d^* = \hat{K}_p e + \hat{K}_I \int e dt \quad (7)$$

where \hat{K}_p and \hat{K}_I define the adaptive proportional and integral control parameters, respectively. In equation (5), V_{dc}^* derived from P&O-based MPPT control and is utilized as a set point for voltage control, and the adaptive law mechanisms of the ARPI voltage control parameters are defined as follows:

$$\dot{K}_P = \mu_1 \times (V_{dc}^* - V_{dc}) \times \frac{1}{1 + |V_{dc}^* - V_{dc}|} \quad (8)$$

$$\dot{K}_I = \mu_2 \int \frac{(V_{dc}^* - V_{dc})}{1 + |V_{dc}^* - V_{dc}|} dt$$

where μ_1 and μ_2 are positive constants in the adaptation scheme. These updated control parameters enable the dc-link voltage to return to the pre-fault conditions, where the error steady-state between V_{dc}^* and V_{dc} is almost zero voltage error.

4. Submission Results and Discussions

To verify the validity of the proposed control approach, consider the 250-kW single-stage three-phase PV system given in Fig.1, which was simulated in Matlab/Simulink environment. Various case simulation scenarios applied to the given system, aim to test the enhancement and capability of the dc-link voltage using the ARPI controller, and hence, they are compared with the results of GW-PI controller as outlined in Table 1.

The results, including three simulation scenarios, are implemented and discussed below.

- Scenario1: effects of environmental changes.
- Scenario2: effects of environmental changes along with the three-phase grid faults.
- Scenario3: effects of environmental changes along with the grid voltage dips.

In Fig.7, irradiance variations are between $1000W/m^2$ and $200W/m^2$. Similarly, the temperature variations vary between $45^\circ C$ and $7^\circ C$. Moreover, the adaptation mechanisms are selected as $\mu_1 = 1$ and $\mu_2 = 1$.

Table 2. Parameters of the conventional PI controllers for the voltage regulation and current regulation.

PI control parameters	Voltage controller	Current controller 1	Current controller 2
K_P	2	3	3
K_I	400	20	20

Table 3. Specifications of the PV panel.

Parameters	Values
dc-link capacitors	0.0543 F
dc-link voltage	480 V
switching frequency	1980 Hz
grid frequency	60 Hz
output voltage of inverter (rms)	3-phase, 250 V
grid voltage	40 kV
filter RL	37.45mΩ, 993.5 mH
transformer nominal power	250 kVA

4.1. Scenario 1: Effects of Environmental Changes.

The effects of variable environmental conditions at the PV pane can subsequently affect the output PV power. Thus, a capability assessment for an overall grid-connected PV

power plant is required under the effects of environmental conditions, particularly to ensure the power balance between the output PV power and grid power.

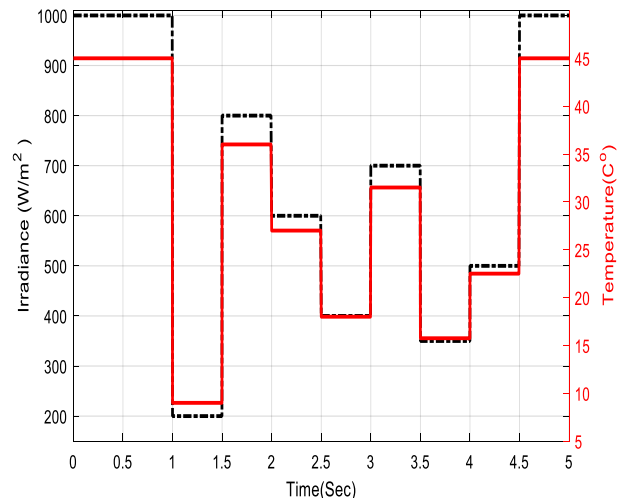


Fig.7. Environmental conditions of solar irradiance and temperature.

Figure 7 obviously demonstrates the variations in solar irradiance and temperature over time. The MPPT has been obtained through these measurements of continuous variations. The PV current is reduced when irradiance decreases and vice versa as plotted in Fig 8a. The output power result from the PV fluctuated because of the effects of irradiance and temperature on PV current and voltage as shown in Fig 8b. Thus, the output PV power is eventually decreased and increased according to the irradiance levels. Figure 8c describes the performance of the dc link voltage regulation during continuous environmental variations and shows that a satisfactory performance was accomplished by the ARPI control strategy. A better transient response of the dc-link voltage is observed under the ARPI controller and less overshoot and ripples are observed compared to the dc-link voltage controlled by the PI controller. Figure 8c also shows that the performance of the dc-link voltage regulated by the PI controller seems to show a sluggish response to DLVR and generates higher overshoot than the dc-link voltage controlled by the ARPI controller. The significance of this finding is that the dc-link voltage based-ARPI controller guarantees a faster and smoother transient performance over random variations of solar irradiance and temperature. Furthermore, Figure 8d-e shows that the voltage at the PCC and grid power have been indirectly affected by continuous weather variations that are subject to PV panels.

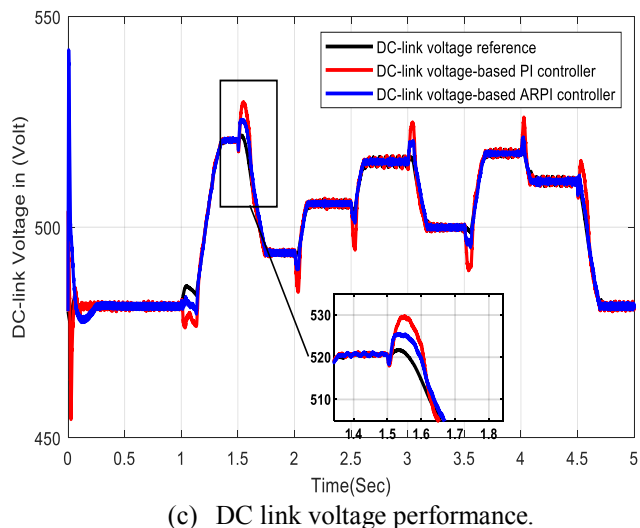
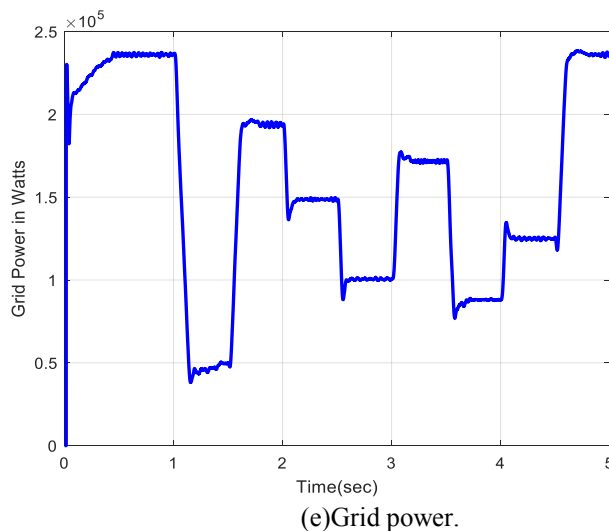
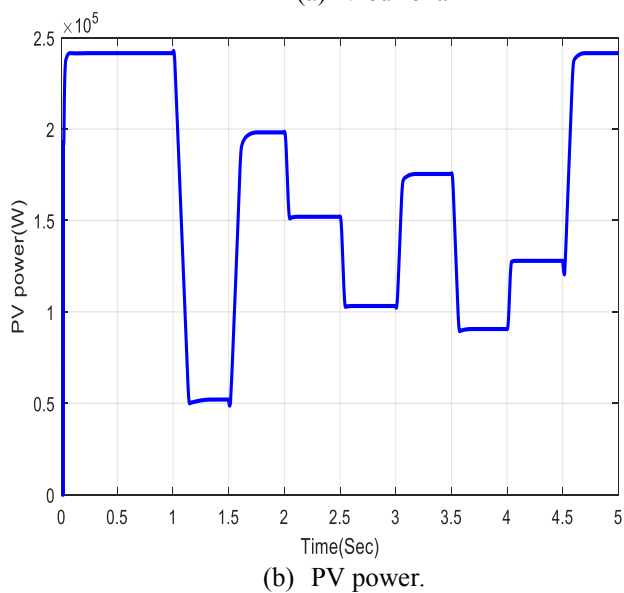
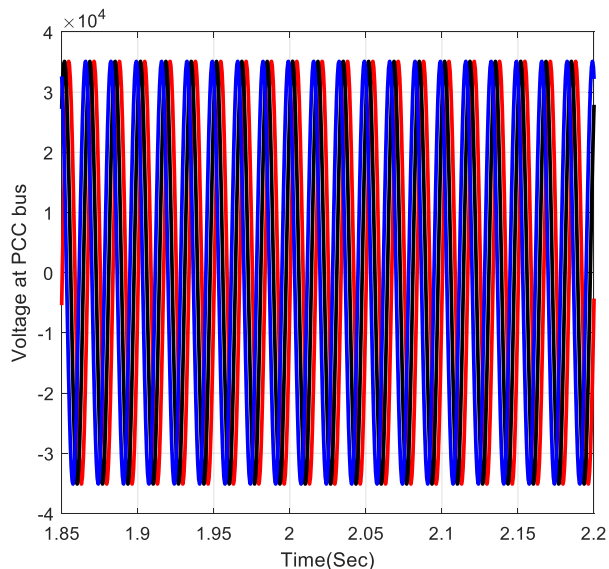
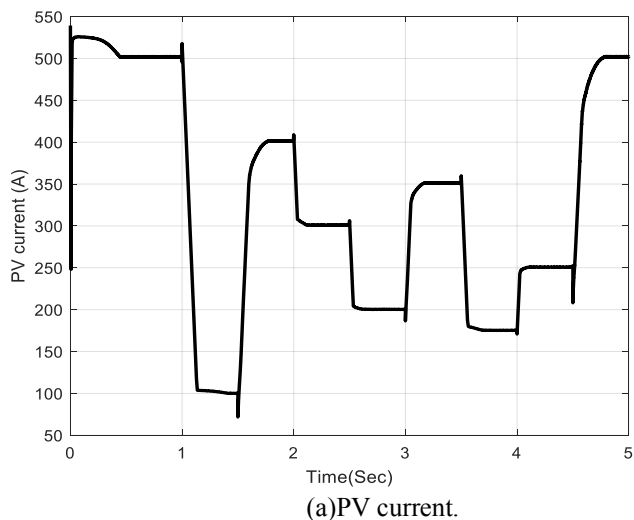


Fig. 8. Performance results over random solar irradiance and temperature.

4.2 Scenario 2: Effects of Environmental Changes along with Three-Phase Grid Faults.

The capability assessment of the ARPI controller implemented in the voltage control scheme is performed based on symmetrical three-phase short-circuit faults at 1.9 sec to 2 sec at the PCC under continuous weather changes as shown in Fig 7.

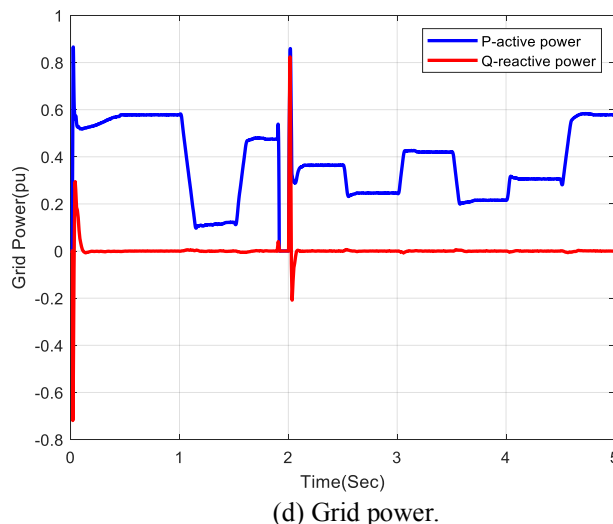
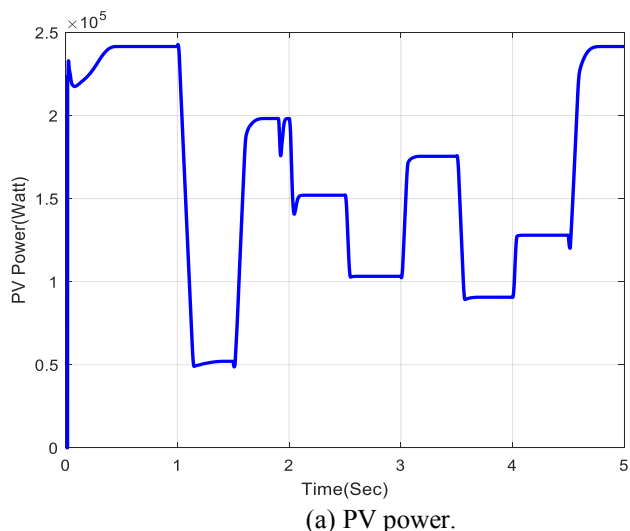
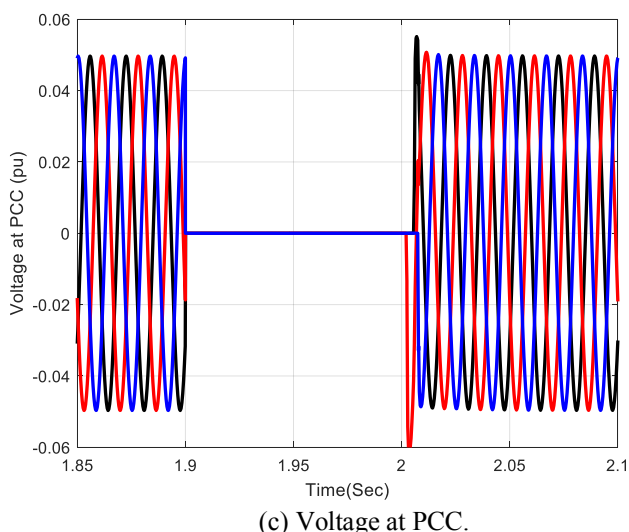
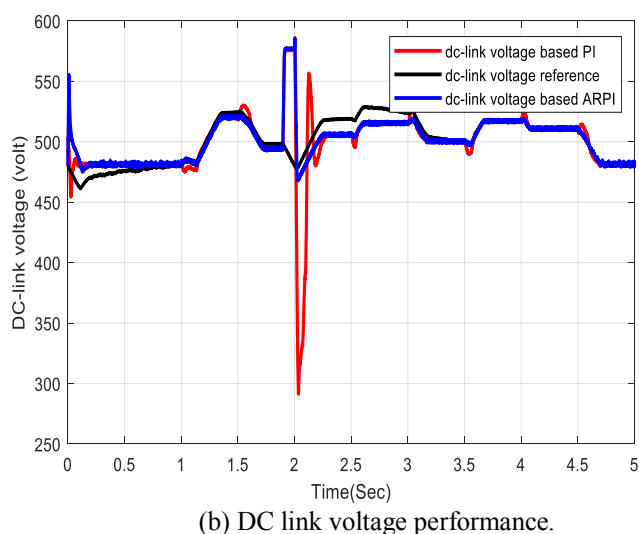


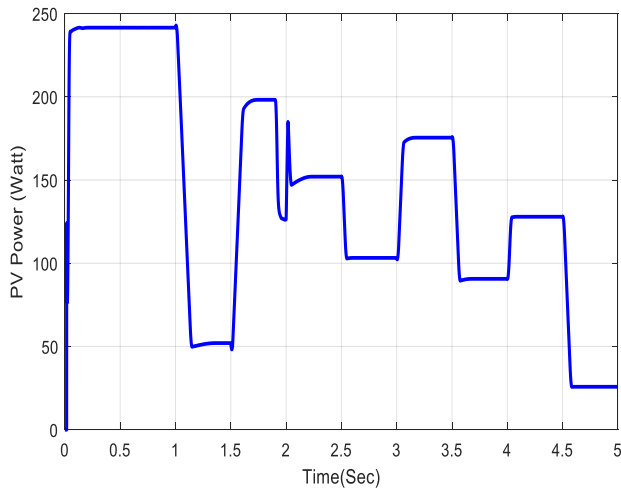
Fig.9. Performance results of the three-phase short-circuit test under environmental changes.



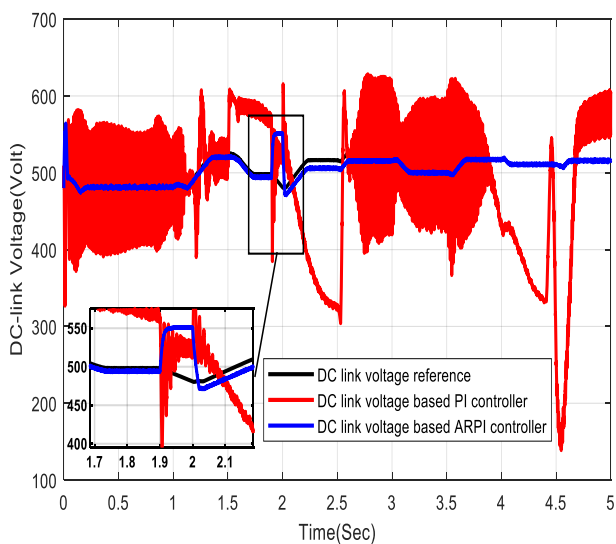
The simulation results that are shown in Fig.9 illustrate the effects of simultaneous weather changes and symmetrical three-phase short-circuit faults from 1.9 sec to 2 sec. at PCC bus. As shown in Fig.9a, the impacts of environmental changes as the main inputs to the PV array were reflected in a continuous reduction of PV power. In the single-stage inverter topology, the output MPPT controller is directly connected to the inverter, where it is fully utilized as the DLVR. In normal operation, the dc-link voltage tracks the DLVR under atmospheric change. However, Figure 9b shows that during the grid faults, the impact on the DLVR was consistent with the impact on the MPPT in a single-stage grid-connected PV inverter. As the DLVR has been limited by a specific range between 357 and 583 volts in the MPPT algorithm, the MPPT voltage which represents the DLVR was decreased while the actual dc-link voltage controlled by the PI and ARPI were most likely increased to the maximum voltage reference rate. Additionally, the PI controller is not as effective as the ARPI controller used in dc-link voltage regulation. Also, dc-link voltage based on the PI controller gained higher overshoot compared to the dc-link based on the ARPI controller, which is less sensitive to the short-circuit faults from 1.9 sec to 2 sec. Thus, the proposed ARPI has enhanced the actual dc-link voltage to rapidly return and track the DLVR in order to maintain a better balance between the generated PV power and grid power after fault clearance. Moreover, three-phase short circuit occurred at PCC bus has been depicted in Fig.9c, the PCC voltage decreased to zero voltage from 1.9 sec to 2 sec until three-phase short-circuit was cleared at 2 sec, and then the PCC voltage returned to its pre-short-circuit fault condition under continuous effects of environmental conditions. This indicates that the PCC voltage was not only regulated, but also returning to pre-fault condition when the ARPI controller was applied. In Fig. 9d, the grid power was clearly interrupted by short-circuit faults from 1.9 sec to 2 sec. As a result, active power increased drastically and reactive power started compensating at 1.9 sec. eventually, when three-phase fault was cleared, and both active and reactive power returned to pre-short-circuit fault conditions as under continuous atmospheric change.

4.3 Scenario 2: Effects of Environmental Changes along with Voltage dips.

Causes of the voltage dip in a grid-connected PV system results from nonlinear load variations and large load connections. As a result, this 50% voltage dip led to the reduction of active power into the grid, oscillation of the output voltage and distortion of the output current.



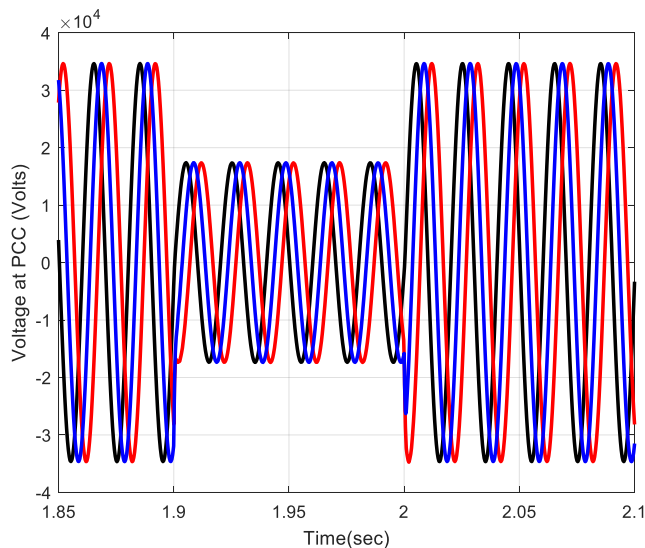
(a) PV power.



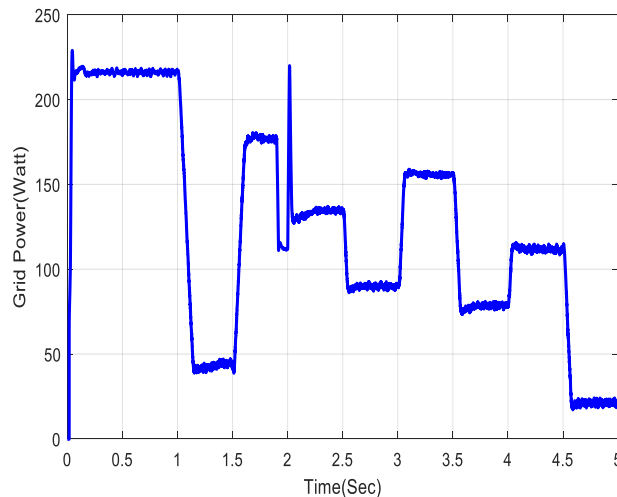
(b) DC link voltage performance.

The performance results of the single-stage PV system during environmental change simultaneous within a 50% sudden voltage dip from 1.9 sec to 2 sec are demonstrated in Fig 10. In Fig.10a, the effects of environmental conditions at the PV panel lead to continuous reductions in PV power. In the single-stage grid-connected PV inverter topology, the output MPPT is directly connected to the inverter so that it can be fully employed as the DLVR. During normal operations, the actual dc-link voltage tracks the desired dc-link voltage reference with a zero-error steady state; thus, a balance was achieved between the generated PV power and grid demand. However, during a sudden voltage dip, extra energy was stored as dc-link capacitance; thus, the dc-link voltage increased, and then the PV power was decreased because the operating point on V-I characteristics was shifted to the open-circuit voltage rate, which caused a reduction in

the PV current. This finding explicitly indicates that a single stage inverter has a self-protection strategy. In addition, Figure 10b shows that the actual dc-link voltage controlled by the ARPI controller increased at the fault occurrence and then rapidly returned to the DLVR as closely as possible after the voltage dip clearance with less overshoot. On the other hand, the dc-link voltage regulated by the PI controller that is sensitive to disturbance showed undesired performance under different weather conditions along with voltage dip. Also, it deviated from the DLVR for a long period of time after the voltage dip had vanished.



(c) Voltage at PCC.



(d) Grid power.

Fig.10. Performance results for environmental changes within a 50% voltage dip.

It is worth mentioning that the tracking error between the DLVR and actual dc-link voltage controlled by the ARPI ensured the stability of the dc-link voltage and maintains the best power balance. As described in Fig.10c, PCC voltage decreased 50 % of its amplitude at 1.9 sec until the dipping condition released from the grid at 2 sec with continuous environmental changes. This indicates that the PCC voltage was not only regulated, but also returning to pre fault condition when the ARPI controller was applied. Similarly,

Figure 10d shows that the grid power was reduced by the id current, which was controlled by the adaptive voltage control under the effects of the voltage dip and environmental changes.

5. Conclusion

The performance of a 250-kW single-stage grid-connected PV inverter was enhanced, and the voltage profile enhancement at PCC between the PV power system and the grid under multiple case simulation scenarios were attained. The achievements of the ARPI controller under environmental change, three-phase fault and voltage dip, effectively enhanced the transient stability performance of the dc-link voltage and its static response with zero steady-state error. Therefore, the power balance was between PV power and grid power was ensured. Moreover, the PCC voltage was disturbed by different disturbance scenarios, but was able to return promptly to pre-fault conditions.

Acknowledgements

Authors may acknowledge to any person, institution or department that supported to any part of study.

References

- [1] B. Singh, S. Kumar and C. Jain, "Damped-SOGI-Based Control Algorithm for Solar PV Power Generating System", *IEEE Transactions on Industry Applications*, vol. 53, no. 3, pp. 1780-1788, May-June 2017.
- [2] P. Wu, W. Huang and N. Tai, "Novel grid connection interface for utility-scale PV power plants based on MMC", *The Journal of Engineering*, vol. 2019, no. 16, pp. 2683-2686, April 2019.
- [3] Y. Chen and K. M. Smedley, "A cost-effective single-stage inverter with maximum power point tracking", in *IEEE Transactions on Power Electronics*, vol. 19, no. 5, pp. 1289-1294, Sept 2004.
- [4] M. M. Hashempour, M. Yang and T. Lee, "An Adaptive Control of DPWM for Clamped-Three-Level Photovoltaic Inverters With Unbalanced Neutral-Point Voltage", *IEEE Transactions on Industry Applications*, vol. 54, no. 6, pp. 6133-6148, Nov.-Dec. 2018.
- [5] L. Lledo, V. Torralba, A. Soret, J. Ramon, F.J. Doblaz-Reyes, "Seasonal forecasts of wind power generation", *Renewable Energy*, No 143, pp. 91-100, December 2019.
- [6] Y. Yang, P. Enjeti, F. Blaabjerg and H. Wang, "Wide-Scale Adoption of Photovoltaic Energy: Grid Code Modifications Are Explored in the Distribution Grid", *IEEE Industry Applications Magazine*, doi: 10.1109/MIAS.2014.2345837, vol. 21, no. 5, pp. 21-31.
- [7] S. Kouro, J. I. Leon, D. Vinnikov and L. G. Franquelo, "Grid-Connected Photovoltaic Systems: An Overview of Recent Research and Emerging PV Converter Technology", *IEEE Industrial Electronics Magazine*, doi: 10.1109/MIE.2014.2376976, vol. 9, no. 1, pp. 47-61.
- [8] J. C. Hernández, P. G. Bueno and F. Sanchez-Sutil, "Enhanced utility-scale photovoltaic units with frequency support functions and dynamic grid support for transmission systems", *IET Renewable Power Generation*, doi: 10.1049/iet-rpg.2016.0714, Vol. 11, No. 3, pp. 361-372.
- [9] X. Fu, H. Chen, R. Cai and P. Yang, "Optimal allocation and adaptive VAR control of PV-DG in distribution networks", *Applied Energy*, vol.137,pp.173-182, January 2015.
- [10] X. Fu, Q. Fu and W. Tang, "Grid connection technique based on μ theory for a two-stage PV structure", *IET Power Electronics*, vol. 12, no. 6, pp. 1545-1553, 29 5 2019.
- [11] C. Jain and B. Singh, "A Three-Phase Grid Tied SPV System With Adaptive DC Link Voltage for CPI Voltage Variations", *IEEE Transactions on Sustainable Energy*, vol. 7, no. 1, pp. 337-344, January 2016.
- [12] L. Piegari and R. Rizzo, "Adaptive perturb and observe algorithm for photovoltaic maximum power point tracking", *IET Renewable Power Generation*, vol. 4, no. 4, pp. 317-328, July 2010.
- [13] D. Sera, L. Mathe, T. Kerekes, S. V. Spataru and R. Teodorescu, "On the Perturb-and-Observe and Incremental Conductance MPPT Methods for PV Systems", *IEEE Journal of Photovoltaics*, vol. 3, no. 3, pp. 1070-1078, July 2013. (Article)
- [14] A. Brambilla, M. Gambarara, A. Garutti and F. Ronchi, "New approach to photovoltaic arrays maximum power point tracking", *30th Annual IEEE Power Electronics Specialists Conference. Record. (Cat. No.99CH36321)*, Charleston, SC, USA, pp. 632-637, vol.2. 1-1 July 1999
- [15] D. P. Hohm and M. E. Ropp, "Comparative study of maximum power point tracking algorithms using an experimental, programmable, maximum power point tracking test bed", *Conference Record of the Twenty-Eighth IEEE Photovoltaic Specialists Conference - 2000 (Cat. No.00CH37036)*, Anchorage, AK, USA, pp. 1699-1702. 15-22 Sept. 2000.
- [16] W. Swiegers and J. H. R. Enslin, "An integrated maximum power point tracker for photovoltaic panels", *IEEE International Symposium on Industrial Electronics. Proceedings. ISIE'98 (Cat. No.98TH8357)*, Pretoria, South Africa, pp. 40-44, 7-10 July 1998.
- [17] M. G. Batarseh and M. E. Za' ter, "A MATLAB Based Comparative Study between Single and Hybrid MPPT Techniques for Photovoltaic Systems", *International Journal of Renewable Energy Research*, Vol.9, No.4, December 2019.
- [18] Y. Shaiek, M. B. Smida, A. Sakly and M. F. Mimouni, "Comparison between conventional methods and GA approach for maximum power point tracking of shaded solar PV generators", *Solar Energy*, vol. 90, pp. 107-22, April 2013.
- [19] B. N. Alajmi, K. H. Ahmed, S. J. Finney and B. W. Williams, "Fuzzy-Logic-Control Approach of a Modified Hill-Climbing Method for Maximum Power Point in Microgrid Standalone Photovoltaic System", *IEEE Transactions on Power Electronics*, vol. 26, no. 4, pp. 1022-1030, April 2011.

- [20] M.I. Mosaad, M.O. El-Raouf, M.A. Al-Ahmar and F.A. Banakher, "Maximum Power Point Tracking of PV system Based Cuckoo Search Algorithm; review and comparison", *Energy Procedia*, vol. 162, pp. 117-126, April 2019.
- [21] M.O.A. El-Raouf, M.I. Mosaad, A. Mallawany, M.A. Al-Ahmar and F.M.E. Bendary, "MPPT of PV-Wind-Fuel Cell of Off-Grid Hybrid System for a New Community", *2018 Twentieth International Middle East Power System Conference (MEPCON)*, Cairo, Egypt, 2018, pp.480-487.
- [22] S.A. Rizzo and G. Scelba, "ANN based MPPT method for rapidly variable shading conditions", *Applied Energy*, vol.145, pp.124-132, May 2015.
- [23] W. Libo, Z. Zhengming and L. Jianzheng, "A Single-Stage Three-Phase Grid-Connected Photovoltaic System With Modified MPPT Method and Reactive Power Compensation", *IEEE Transactions on Energy Conversion*, vol. 22, no. 4, pp. 881-886, Dec. 2007.
- [24] F.Gao, D. Li, P. C. Loh, Y. Tang and P. Wang, "Indirect dc-link voltage control of two-stage single-phase PV inverter", *2009 IEEE Energy Conversion Congress and Exposition*, San Jose, CA, 2009, pp. 1166-1172.
- [25] M. S. El Moursi, W. Xiao and J. L. Kirtley, "Fault ride through capability for grid interfacing large scale PV power plants", *IET Generation, Transmission & Distribution*, vol. 7, no. 9, pp. 1027-1036, Sept. 2013.
- [26] R. N. Tripathi and T. Hanamoto, "FRIT based optimized PI tuning for DC link voltage control of grid connected solar PV system", *IECON 2015 - 41st Annual Conference of the IEEE Industrial Electronics Society*, Yokohama, 2015, pp. 001567-001572.
- [27] P. Mishra, A. K. Pradhan and P. Bajpai, "Voltage control of PV inverter connected to unbalanced distribution system", *IET Renewable Power Generation*, vol. 13, no. 9, pp. 1587-1594, 8 7 2019.
- [28] M.Mosaad, N.Elkalashy, and M.Ashmawy, "Integrating adaptive control of renewable distributed switched reluctance generation and feeder protection coordination", *Electric Power System Research*, 154, 452-462, 2018.
- [29] M. Mosaad, "Model reference adaptive control of STATCOM for grid integration of wind energy systems", *IET Electric Power Applications*, 2018, 12, 5, 605 - 613, 2018.
- [30] C. Jain and B. Singh, "Single-phase single-stage multifunctional grid interfaced solar photo-voltaic system under abnormal grid conditions", *IET Generation, Transmission & Distribution*, vol. 9, no. 10, pp. 886-894, 2 7 2015.
- [31] F. A. S. Neves, M. Carrasco, F. Mancilla-David, G. M. S. Azevedo and V. S. Santos, "Unbalanced Grid Fault Ride-Through Control for Single-Stage Photovoltaic Inverters", *IEEE Transactions on Power Electronics*, vol. 31, no. 4, pp. 3338-3347, April 2016.
- [32] H. Ghoddami and A. Yazdani, "A Single-Stage Three-Phase Photovoltaic System With Enhanced Maximum Power Point Tracking Capability and Increased Power Rating", *IEEE Transactions on Power Delivery*, vol. 26, no. 2, pp. 1017-1029, April 2011.
- [33] V. N. Lal and S. N. Singh, "Control and Performance Analysis of a Single-Stage Utility-Scale Grid-Connected PV System", *IEEE Systems Journal*, vol. 11, no. 3, pp. 1601-1611, Sept. 2017.
- [34] D.H. Hwang, J.Y. Lee, and Y. Cho, "Single-phase single-stage dual-buck photovoltaic inverter with active power decoupling strategy", *Renewable energy*, vol.126, pp. 454-464, October 2018.
- [35] G.Yan, J. Ren, G. Mu, L. Jin, S. Duan and Q. Jia, "DC-link voltage stability analysis for single-stage photovoltaic VSIs connected to weak grid", *2016 IEEE 8th International Power Electronics and Motion Control Conference (IPEMC-ECCE Asia)*, Hefei, 2016, pp. 474-478.
- [36] M. Mirhosseini, J. Pou and V. G. Agelidis, "Single- and Two-Stage Inverter-Based Grid-Connected Photovoltaic Power Plants With Ride-Through Capability Under Grid Faults", *IEEE Transactions on Sustainable Energy*, vol. 6, no. 3, pp. 1150-1159, July 2015.
- [37] Qiuwei Wu and Yuanzhang Sun, "Fault Ride Through Enhancement of VSC-HVDC Connected Offshore Wind Power Plants", in *Modeling and Modern Control of Wind Power*, IEEE, 2018, pp.215-231 doi: 10.1002/9781119236382.ch11
- [38] Y. Wang and B. Ren, "Fault Ride-Through Enhancement for Grid-Tied PV Systems With Robust Control", in *IEEE Transactions on Industrial Electronics*, vol. 65, no. 3, pp. 2302-2312, March 2018. doi: 10.1109/TIE.2017.2740858.
- [39] Worku, M.Y., Abido, M.A., 2015. Grid-connected PV array with supercapacitor energy storage system for fault ride through. In: IEEE International Conference on Industrial Technology (ICIT). IEEE, pp. 2901-2906.
- [40] Zeng, D., Guo, J., Ding, M., Geng, D., 2015. Fault-ride-through capability enhancement by adaptive voltage support control for inverter interfaced distributed generation. In: 5th International Conference on Electric Utility Deregulation and Restructuring and Power Technologies (DRPT). IEEE, pp. 1924-1928.
- [41] Lidong Zhan and M. H. J. Bollen, "Characteristic of voltage dips (sags) in power systems", in *IEEE Transactions on Power Delivery*, vol. 15, no. 2, pp. 827-832, April 2000. doi: 10.1109/61.853026.
- [42] G. Ding *et al.*, "Adaptive DC-Link Voltage Control of Two-Stage Photovoltaic Inverter During Low Voltage Ride-Through Operation", in *IEEE Transactions on Power Electronics*, vol. 31, no. 6, pp. 4182-4194, June 2016. doi: 10.1109/TPEL.2015.2469603
- [43] C. Ma, F. Gao, G. He and G. Li, "A Voltage Detection Method for the Voltage Ride-Through Operation of Renewable Energy Generation Systems Under Grid Voltage Distortion Conditions", in *IEEE Transactions on Sustainable Energy*, vol. 6, no. 3, pp.
- [44] Petreus, D, Daraban, S, Ciocan, I, Patarau, T, Morel, C and Machmoum, M, "Low cost single-stage micro-inverter with MPPT for grid connected applications", *Solar Energy*, 92, 241-255, 2013.
- [45] Ding, G., Gao, F., Tian, H., Ma, C., Chen, M., He, G., Liu, Y., "Adaptive DC-link voltage control of two-

stage photovoltaic inverter during low voltage ride-through operation”, *IEEE Trans. Power Electron*, vol 31, pp.4182–4194, 2016.

- [46] Teresa Orłowska-Kowalska, Frede Blaabjerg and José Rodríguez, *Advanced and Intelligent Control in Power*

Electronics and Drives, vol. 531. Springer International Publishing Switzerland, 2014, 410 pages, ISBN: 978-3-319-03400-3.